Journal of Inorganic Biochemistry 192 (2019) 33–44

Contents lists available at ScienceDirect

Journal of Inorganic Biochemistry

journal homepage: www.elsevier.com/locate/jinorgbio

Does phosphorylation increase the binding affinity of aluminum? A computational study on the aluminum interaction with serine and O-phosphoserine

Elena Formoso[a,b,*], Rafael Grande-Aztatzi[b], Xabier Lopez[c,b]

[a] Farmazia Fakultatea, Euskal Herriko Unibertsitatea (UPV/EHU), 01006 Vitoria-Gasteiz, Euskadi, Spain
[b] Donostia International Physics Centre (DIPC), Donostia 20018, Euskadi, Spain
[c] Kimika Fakultatea, Euskal Herriko Unibertsitatea (UPV/EHU), P.K. 1072, 20080 Donostia, Euskadi, Spain

ARTICLE INFO

Keywords:
Density Functional Theory
Aluminum speciation
Phosphorylation
QTAIMs

ABSTRACT

Several toxic effects arise from aluminum's presence in living systems, one of these effects is to alter the natural role of enzymes and non-enzyme proteins. Aluminum promotes the hyperphosphorylation of normal proteins. In order to assess the aluminum-binding abilities of phosphorylated proteins and peptides, the interaction of aluminum at different pH with serine and phosphoserine is studied by a Density Functional Theory study, combined with polarizable continuum models to account for bulk solvent effects, and the electronic structure of selected complexes are analyzed by Quantum Theory of "Atoms in Molecules". Our results confirm the high ability of aluminum to bind polypeptides as the pH lowers. Moreover, the phosphorylation of the building blocks increases the affinity for aluminum, in particular at physiological pH. Finally, aluminum shows a tendency to be chelated forming different size rings.

1. Introduction

Aluminum, the third most abundant metal in the earth's crust, has largely been excluded from biochemical evolution because of its efficient cycling within the lithosphere [1,2]. However, over the last century human intervention (soil acidification, food additives, pharmaceuticals, Al-containers, water treatment, etc.) has increased the availability of biologically reactive aluminum [2]. Unfortunately, there is increasing evidence of the potential toxic effects of aluminum in biological systems [3], linking the presence of aluminum in the human body with several diseases [4-6]. The full molecular basis for aluminum toxicity is still poorly understood, but some potential mechanisms have been outlined. For instance, it has been well established that aluminum shows a significant pro-oxidant activity in biological systems [7-9], it also inhibits the normal function of various enzymes involved in the glycolysis pathway [10-13] and in the production of glutamate [14,15] affecting the TCA cycle [16]. Moreover, several studies have shown that aluminum competes with magnesium as a metal-ATP co-factor [17-20] and that it can modify the electronic and structural properties of the chelated biological ligands [16,21-23].

Aluminum as a strong Lewis acid, hard metal, shows a strong preference for binding negatively-charged oxygen atoms [24]. In fact, citrate, which contains three carboxylates and one alcohol group, is recognized as the main aluminum low molecular mass chelator in blood serum [25]. On the other hand, molecules containing phosphate groups are also a likely target for interacting with the cation [24,26-30]. Due to the variety of cellular processes in which molecules containing phosphate groups are present (ATP, phosphorylated proteins, sugar phosphates, DNA, etc.), this high affinity to form Al(III)–phosphate compounds could disrupt key processes of the cell metabolism [26-28].

Aluminum is considered as a neurotoxic element associated with Alzheimer's disease (AD), but there are controversies and uncertainties on the role that aluminum plays in neurodegeneration [6,31,32]. In a seminal study, Exley et al. demonstrated the ability of aluminum to bind β-amyloids [33], which leads to a switch in structure between the α-helix and β-sheet. Moreover, in vitro experiments determined that Al (III) promotes the aggregation of β-amyloid peptides more efficiently than other metals [34,35], with the main constituent of insoluble amyloid plaques known as senile plaques, and in fact, aluminum has been detected in senile plaques extracted from the brains of patients with AD [36]. In addition, this metal also induces the abnormal neurofilament tangle (NFT) aggregation and promotes the hyperphosphorylation of normal proteins [37,38]. As a matter of fact, phosphorylation of proteins is thought to increase their affinity for

* Corresponding author.
E-mail address: elena.formoso@ehu.eus (E. Formoso).

https://doi.org/10.1016/j.jinorgbio.2018.12.004
Received 3 July 2018; Received in revised form 9 November 2018; Accepted 2 December 2018
Available online 15 December 2018
0162-0134/

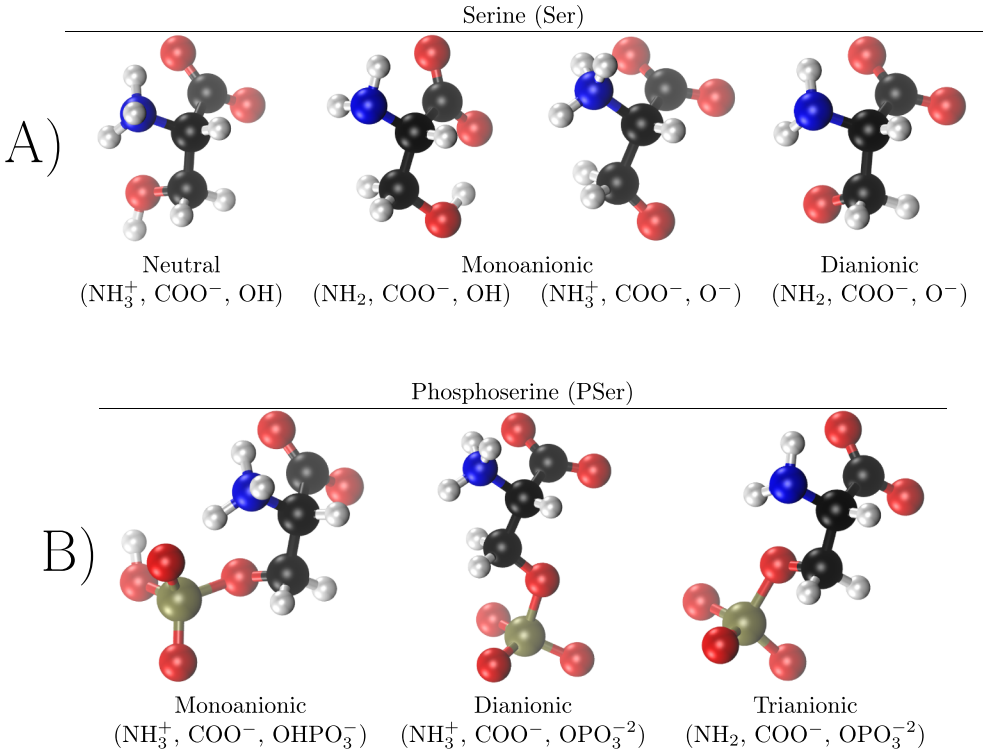

Fig. 1. The two ligands employed in this study, serine and phosphoserine: A) The different ionic species analyzed for serine (Ser) and the titratable groups of each species; B) The different ionic species studied for phosphoserine (PSer) and the titratable groups of each of the species.

aluminum and could be a key aspect in understanding how aluminum promotes the hyperphosphorylation of tau and its aggregation in NFT formation. The alcoholic-OH of serine (Ser) and threonine (Thr) and the phenolic-OH of tyrosine are the phosphorylation sites of proteins. Thus, phosphoserine (PSer) molecule serves as a first step to understand how phosphorylated protein residues can interact with aluminum. In addition, PSer occurs naturally in the human body as an intermediate in the biosynthesis of L-serine, the specific enzyme phosphoserine phosphatase hydrolyzes PSer to L-serine [39].

The aim of this work is to give insight into the increase in the binding affinity of aluminum to phosphorylated proteins in general. As a first step of this goal, we characterize and compare the binding affinity of aluminum cation to serine and phosphorylated serine (PSer), see Fig. 1. We chose this single amino acid system, since it is directly related to the experimental work by Kiss et al. [40], representing the smallest possible phosphorylated peptide. This allows us to estimate the increase in aluminum binding affinity expected by phosphorylation of Ser in peptides. The metal binding abilities of PSer have been previously studied with several 3d transition metal and alkaline earth metal ions by means of potentiometric and NMR measurements [40-42]. In fact, monodentate phosphate coordination was found with Ca (II) and Mg(II), bidentate (NH_2, CO_2^-) coordination with Cu(II), and tridentate (OPO_3^{-2},NH_2, CO_2^-) chelation with Co(II), Mn(II), Ni(II) and Zn(II). In the case of aluminum, Kiss et al. [40] proposed a monodentate phosphate coordination or tridentate (OPO_3^{-2}, NH_2, CO_2^-) chelation. In the present paper, we provide Density Functional Theory (DFT) estimations of the aluminum binding affinity in the context of polarizable continuum models to consider bulk solvent effects for at least 133 Al-Ser and Al-PSer structures (see Fig. 2). This dataset comprises mononuclear Aluminum-Serine and Aluminum-Phosphoserine complexes with various hydrolytic species of aluminum as reference structures ($[Al(H_2O)_6]^{3+}$,$[Al(OH)(H_2O)_5]^{2+}$, and $[Al(OH)_2(H_2O)_4]^{1+}$, which hereafter they will be referred to as Al^{3+}, $[Al(OH)]^{2+}$ and $[Al(OH)_2]^+$ species), and considering various binding modes to the different protonation states of Ser and PSer (see Fig. 1). In addition, we compare our results with previous studies using similar methodologies of well-known aluminum binders in biological media [24] such as citrate, 2,3 − *diphosphoglyceric acid* [43] or glucose 6-phosphate [30].

2. Methods

All geometrical optimizations were carried out in water solution with an Integral Equation Formalism Polarizable Continuum Model (IEFPCM) [44] as implemented in Gaussian09, [45] B3LYP functional [46-49] with D3 version of Grimme's dispersion corrections with Becke-Johnson damping [50] and 6-31 + + G(d,p) basis set. To confirm that the optimized structures were real minima on the potential energy surfaces, frequency calculations were carried out at the same level of theory. All structures showed positive force constants for all the normal modes of vibration. The frequencies were then used to evaluate the zero-point vibrational energy (ZPVE) and the thermal (T = 298 K) vibrational corrections to the enthalpies and Gibbs free energies within the harmonic oscillator approximation. To calculate the entropy, the different contributions to the partition function were evaluated using the standard statistical mechanics expressions in the canonical ensemble and the harmonic oscillator and rigid rotor approximation. The electronic energies were refined by single-point energy calculations at the B3LYP/6-311 + + G(3df,2p) level of theory. The adequacy of this methodology has been proven to show good performance in the trends in binding affinity [16,24,29,30,43]. Nevertheless, to confirm the adequacy of the methodology, we re-evaluated the affinity energies of some representative complexes by single-point calculations with four different functionals: PBE0-D3BJ, TPSS-D3BJ, B97D3 and M06-2X. The trends in binding affinity are equally described by the different functionals. The results can be found in the Supporting Information (SI).

2.1. Binding free energies in solution

We studied at least 133 different 1:1 aluminum-serine and aluminum-phosphoserine complexes. Al^{3+}, $[Al(OH)]^{2+}$, and $[Al(OH)_2]^+$

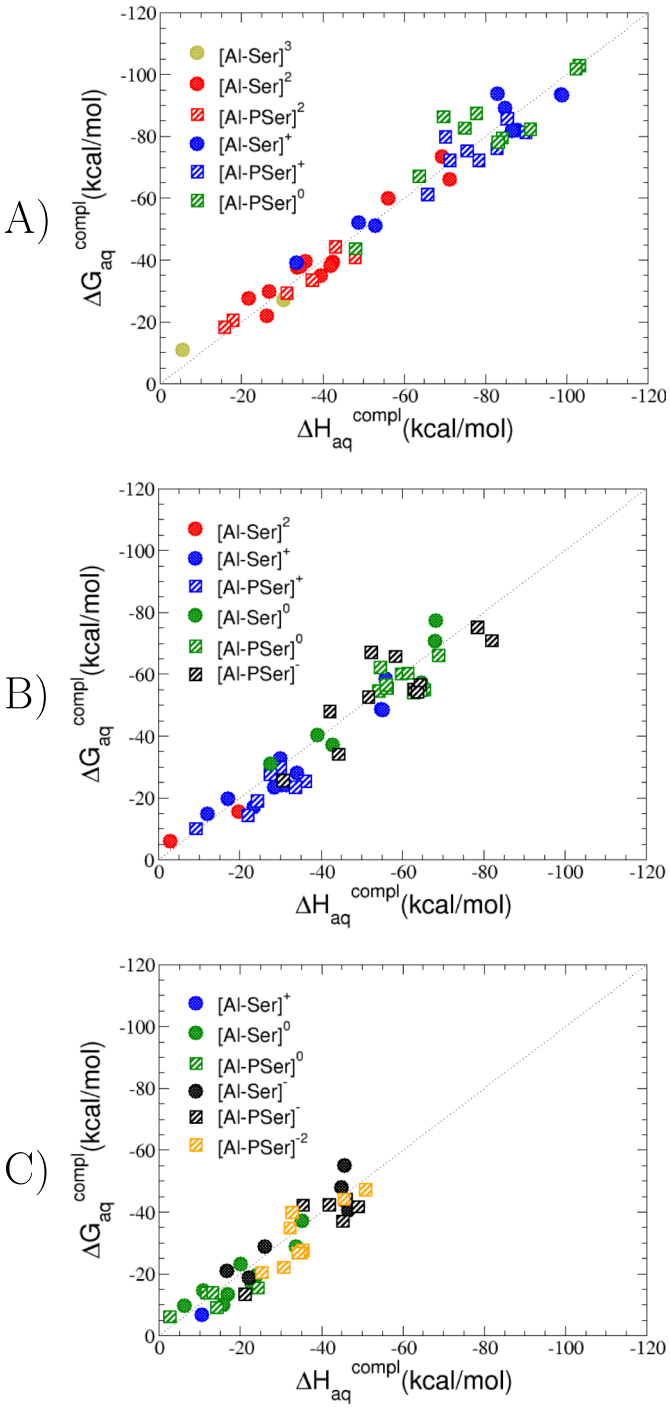

Fig. 2. Complexation enthalpies and free energies for Al-Ser (filled circles) and Al-PSer (striped squares) complexes: A) Al^{3+} complexes; B) $[Al(OH)]^{2+}$ complexes; and C) $[Al(OH)_2]^{1+}$ complexes. The different colors account for the total charge of the complex: +3 (yellow), +2 (red), +1 (blue), 0 (green), −1 (black) and −2 (orange).

hydrolytic species were analyzed with four and three different protonation states for Ser and PSer, respectively. The 1:1 complex formation stability was studied following the ligand substitution reaction shown in Eqs. (1), (2) and (3):

$$[Al(H_2O)_6]^{3+}_{(aq,1\,M)} + L^{q-}_{(aq,1\,M)} \rightarrow [Al(H_2O)_{(6-m)}L]^{3-q}_{(aq,1\,M)} + mH_2O \quad (1)$$

$$[Al(H_2O)_5(OH)]^{2+}_{(aq,1\,M)} + L^{q-}_{(aq,1\,M)} \rightarrow [Al(OH)(H_2O)_{(5-m)}L]^{2-q}_{(aq,1\,M)} + mH_2O \quad (2)$$

$$[Al(H_2O)_4(OH)_2]^{1+}_{(aq,1\,M)} + L^{q-}_{(aq,1\,M)} \rightarrow [Al(OH)_2(H_2O)_{(4-m)}L]^{1-q}_{(aq,1\,M)} + mH_2O \quad (3)$$

where q is the net charge of the ligand anion L, and m depends on the ligand's coordination mode to aluminum and can be m = 1, 2, 3 or 4 when the ligand binds in a monodentate, bidentate/dicoordinate, tridentate or tetradentate fashion, respectively. The enthalpy in solution corresponding to the binding of the ligand to Al^{3+} is therefore calculated as:

$$\Delta H^{compl}_{aq} = H_{aq}(Al(H_2O)_{(6-m)}L) + mH_{aq}(H_2O) - H_{aq}(Al(H_2O)_6) - H_{aq}(L) + \Delta nRTln(24.46) \quad (4)$$

Since the enthalpies are determined using an ideal gas at 1 atm as the standard state, the last term in Eq. (4) corresponds to the volume change due to the transformation from 1 atm to 1 M in solution, where Δn refers to the change in the number of species in the reaction [51]. In a similar way, the free energy of the complexes is determined as:

$$\Delta G^{compl}_{aq} = G_{aq}(Al(H_2O)_{(6-m)}L) + mG_{aq}(H_2O) - G_{aq}(Al(H_2O)_6) - G_{aq}(L) + \Delta nRTln(24.46) + mRTln(55.34) \quad (5)$$

where the last term is the entropic factor that accounts for the concentration of 55.34 M of water in liquid water [51].

The enthalpy and free energy in solution corresponding to the binding of the ligand to $[Al(OH)]^{2+}$ and $[Al(OH)_2]^{+}$ are coherent with Eqs. (4) and (5) with the corresponding changes.

The pK_a values for Ser are 2.13, 9.05 and ~13.0, for the carboxylic, amine and alcoholic group, respectively [52], and the values for PSer are ~ 1 (OH_2PO_3), 2.1 ($COOH$), 5.78 ($OHPO_3^-$) and 9.85 (NH_3^{+1}) [53]. In Eqs. (4) and (5) the same protonation state was considered for Ser or PSer in solution and coordinated to aluminum, therefore a correction must be introduced when necessary. In such cases the pK_a values stated above were considered to evaluate the protonation and deprotonation energies as:

$$\Delta G^{deprot} = 2.303RT(pK_a - pH) \quad (6)$$

$$\Delta G^{prot} = 2.303RT(pH - pK_a) \quad (7)$$

where pK_a is the value of the de/protonated group of Ser or PSer and pH is the environmental pH, namely 7.4. The reference pK_a values and the $\Delta G^{deprot}/\Delta G^{prot}$ are shown in Table 1.

The final free energy at physiological pH values (ΔG^{Phys}_{aq}) for all compounds is therefore evaluated as:

$$\Delta G^{Phys}_{aq} = \Delta G^{compl}_{aq} + \Delta G^{deprot} + \Delta G^{prot} \quad (8)$$

2.2. Quantum Theory of Atoms in Molecules

Quantum Theory of " Atoms in Molecules "(QTAIM) [54] was applied to previous geometrically optimized structures. QTAIM

Table 1
Calculated free energies (ΔG^{deprot} and ΔG^{prot}, in kcal/mol) required to de/protonate a titrable group determined according to Eqs. (6) and (7). † taken from ref. [52], and $ taken from ref. [53].

Molecule	Group	pK_a	ΔG^{deprot}	ΔG^{prot}
Ser†	OH	13.0	7.64	
	NH_3^+	9.05	2.25	
PSer$	NH_3^+	9.85	3.34	
	$OHPO_3^-$	5.78		2.21

calculations were carried out with the use of AIMAll v13.05.06 program [55]. The characteristics of bond critical points (BCPs) were analyzed.

The analysis of BCP provides information on the nature of interatomic interaction. For shared interactions like covalent and polarized bonds the Laplacian of electron density ($\nabla^2\rho(r_{BCP})$) is negative since there is concentration of electron density in the atom-atom region. For the interactions between closed-shell systems like van der Waals interactions, ionic ones and hydrogen bonds there is the depletion of electron charge within the atom-atom region that results in low $\rho(r_{BCP})$ and the positive value of Laplacian.

However it was pointed out that for some interactions which may be classified as covalent bonds, the Laplacian is positive and the negative value of the total electron energy density at BCP ($H(r_{BCP})$) is the sufficient criterion of covalency. Such a situation is often observed for strong A—H...B hydrogen bonds classified as partly covalent in nature ($H(r_{BCP})$ negative at H...B BCP), even for very strong hydrogen bonds the Laplacian of the electron density at BCP is negative (like for FHF^- anion where $\nabla^2\rho(r_{BCP})$ for both H...F contacts is negative). However usually, as for the other closed-shell interactions, for A—H...B hydrogen bonds both values, $\nabla^2\rho(r_{BCP})$ and $H(r_{BCP})$, are positive.

The figures were rendered using the VMD software [56] while the graphs were generated using grace v5.1.23.

3. Results and discussion

Ser and PSer have three functional groups able to coordinate the aluminum cation. Carboxylate (COO^-) and amine (NH_3^+) groups are commom in both ligands, while an alkoxide (O^-) group is presented in Ser which is converted to a phosphate (OPO_3^{2-}) group in PSer. Four and three different ionic species for Ser and PSer, respectively, have been analyzed taking into account the pK_a values of each ligand (see Fig. 1). Although, the deprotonation of the alcoholic OH group of Ser would occur in principle at highly alkaline pH range, ~ 13, it is well known that the acidity of the ligand can change upon its coordination to aluminum, so it cannot be neglected [22] . In addition, the coordination to aluminum by the different functional groups of Ser/PSer's ionic species is analyzed. Three different aluminum hydrolytic species are studied, which corresponds to *i*) $[Al(H_2O)_6]^3$ (named Al^{3+} hereafter); *ii*) $[Al(H_2O)_5(OH)]^2$ (named $[Al(OH)]^{2+}$ hereafter); and *iii*) $[Al(H_2O)_4(OH)_2]^{+1}$ (named $[Al(OH)_2]^+$ hereafter). This allows us to study the effect of OH^- in the binding affinity of aluminum by the ligands. As one can see in Fig. 2, the charge is a driving factor for the binding affinity in each aluminum oxidation state, obtaining the largest complexation free energies for the highest negatively charged complexes.

We start analyzing the results of complexes formed by Al^{3+}, followed by $[Al(OH)]^{2+}$ and finish with $[Al(OH)_2]^+$ compounds.

3.1. Al^{3+} species

The formation of various aluminum-serine and aluminum-phosphoserine complexes is studied taking into account the pK_a values of Ser and PSer. The coordination of aluminum by the different functional groups (alkoxide, phosphate, carboxylate and amine groups) is compared in the studied ionic species of Ser and PSer.

A total of 24 Al^{3+}-Ser complexes are analyzed with various total charges, +3, +2 and +1 (see Fig. 2A and SI). As expected, the charge is the driving factor for the binding affinity, obtaining the largest complexation energies for the less positively charge complexes, +1, (see Table 2 and Fig. 2A). On the other hand, the mono- and bidentate binding mode of carboxylate group (Fig. 3 a and 3b) is analyzed in the four possible ionic species of Ser, being the monodentate binding mode, mC, favored against the bidentate one, bC, by at least 7 kcal/mol depending on the ionic species (see Table 2 and SI).

Regarding +2 charge Al-Ser complexes, the structures with NH_3^+ and O^- functional groups show larger complexation free energies than their tautomers with NH_2 and OH groups, even at physiological pH despite the larger penalty in the complexation free energy due to the deprotonation of the alcohol group in the first type of compounds (see Table 1). Besides, the dicoordinate binding mode of carboxylate and alkoxide/amine groups, dCO/dCN, is the preferred chelation mode in both ionic species, ΔG_{aq}^{Phys}= −65.57 kcal/mol and −37.29 kca/mol, respectively (see Fig. 3 d and 3f). Six and five membered rings are formed with those binding motifs, respectively. Moreover, it should be mentioned that the coordination of Al^{3+} by alkoxide presents a higher complexation free energy than the dicoordinate binding by carboxylate and amine groups (dCN), ΔG_{aq}^{Phys}= −58.27 kcal/mol vs −37.29 kcal/mol.

Finally, the tricoordinate binding mode by the three functional groups (tCNO), which forms a (6+5+5)-membered joint rings (see Fig. 3h), is the preferred coordination mode in $[Al\text{-}Ser]^{+1}$ complexes, ΔG_{aq}^{Phys}= −83.84 kcal/mol, followed by the dicoordinate binding mode of carboxylate and alkoxide groups (dCO, ΔG_{aq}^{Phys}= −79.05 kcal/mol) and by alkoxide coordination (ΔG_{aq}^{Phys}= −71.91 kcal/mol). The monodentate binding mode of carboxylate also presents a high complexation free energy (ΔG_{aq}^{Phys}= −83.41 kcal/mol), although it must be noted that a spontaneous proton transfer from a water molecule to the alkoxide group is observed during the geometry optimization process in $[Al\text{-}Ser]^{+1}$ complex, see Fig. 3g. This could be either an artifact of our reduced solvation model, or a real possibility. Notice that the pKa of a water molecule bound to aluminum is 5.3, whereas the pKa of an alkoxide is ~ 13. A partial estimation of the energy associated with this proton transfer revealed that its presence does not alter the main qualitative trends in binding affinities outlined in this article.

To sum up, the binding motifs of Ser to Al^{3+} can be classified in the next decreasing binding affinity order: tricoordinate binding by the three functional groups (COO^-, NH_2, O^-), tCNO ≥ monodentate binding by carboxylate group with proton transfer from a water molecule to alkoxide, mC > dicoordinate binding by carboxylate and alkoxide, dCO > coordination by alkoxide, O > dicoordinate binding by carboxylate and amine, dCN ≥ monodentate binding by carboxylate, mC > bidentate binding by carboxylate, bC > coordination by amine, N.

On the other hand, a total of 24 Al^{3+}-PSer complexes are analyzed with total charges of +2, +1 and 0 (see Fig. 2A and SI). The smallest complexation free energies are obtained for +2 complexes, whereas +1 and 0 charge systems present quite similar complexation free energies, being favored the neutral complexes. Thus, the charge is a driving factor for the binding affinity, as expected from our previous studies of aluminum-biophosphate complexes [24,30,43]. In addition, monodentate binding mode of carboxylate or phosphate groups is preferred against the bidentate ones, see Table 2 and Fig. 4a–d. Moreover, the highest complexation free energy is obtained in $[Al\text{-}PSer]^0$ compounds for the dicoordinate binding of Al^{3+} by carboxylate and phosphate groups (dCP, ΔG_{aq}^{compl}= −102.74 kcal/mol), which forms a 8-membered ring. Note, that in this structure we observe a spontaneous proton transfer from a water molecule to the phosphate group during the geometry optimization process, Fig. 4g. This could be either an artifact of our reduced solvation model, either a real possibility due to the fact that the pKa of a water molecule bound to aluminum is 5.3, whereas the second pKa of the phosphate is ~ 5.78.

$[Al\text{-}PSer]^0$ compounds are able to form two, three and even four joint ring systems with similar complexation free energies. The tricoordinate binding of Al^{3+} by carboxylate monodentately and bidentately by phosphate, tCP, forms a (8+4)-membered joint rings, ΔG_{aq}^{compl}= −87.36 kcal/mol (Fig. 4h), the tridentate chelation by the three functional groups (COO^-, NH_2, OPO_3^{-2}, tCNP) forms (8+7+5)-membered joint rings, ΔG_{aq}^{compl}= −82.53 kcal/mol (Fig. 4i), while the tetracoordinate binding by the three functional groups with the phosphate in a bidentate fashion, tCNbP, forms (8+7+5+4)-membered joint rings, ΔG_{aq}^{compl}= −86.20 kcal/mol (Fig. 4j). It should be mentioned that the dicoordinate binding of Al^{3+} by carboxylate and phosphate groups,

Table 2
Enthalpy and free energy affinities in kcal/mol for Al^{3+} − *Ser/PSer* complexes formation with corrections that account for the physiological pH and de/protonation of the corresponding titratable groups. The subscripts indicate the coordination mode of Ser/PSer to Al^{3+}. The † sign indicates a spontaneous proton transfer from a water molecule to alkoxide/phosphate group during the optimization. The ‡ sign indicates two spontaneous proton transfer from a water molecule to the phosphate group and from another water molecule to carboxylate group during the optimization.

	Titratable groups	Structure	ΔH_{aq}^{compl}	ΔG_{aq}^{compl}	ΔG_{aq}^{Phys}
$Al^{3+} - Ser$	NH_3^+, OH	$[Al(Ser)_{mC}(H_2O)_5]^3$	-30.38	-27.01	-27.01
		$[Al(Ser)_{bC}(H_2O)_4]^3$	-5.57	-10.69	-10.69
	NH_3^+, O^-	$[Al(Ser)_{bC}(H_2O)_4]^2$ (†)	-56.18	-59.71	-52.06
		$[Al(Ser)_{O}(H_2O)_5]^2$	-71.21	-65.91	-58.27
		$[Al(Ser)_{dCO}(H_2O)_4]^2$	-69.36	-73.21	-65.57
	NH_2, OH	$[Al(Ser)_{mC}(H_2O)_5]^2$	-42.47	-39.29	-37.04
		$[Al(Ser)_{bC}(H_2O)_4]^2$	-26.77	-29.66	-27.41
		$[Al(Ser)_{N}(H_2O)_5]^2$	-26.37	-21.93	-19.68
		$[Al(Ser)_{dCN}(H_2O)_4]^2$	-35.87	-39.54	-37.29
	NH_2, O^-	$[Al(Ser)_{mC}(H_2O)_5]^1$ (†)	-98.69	-93.31	-83.41
		$[Al(Ser)_{bC}(H_2O)_4]^1$	-33.50	-38.97	-29.08
		$[Al(Ser)_{O}(H_2O)_5]^1$	-87.95	-81.80	-71.91
		$[Al(Ser)_{dCO}(H_2O)_4]^1$	-84.86	-88.95	-79.05
		$[Al(Ser)_{dCN}(H_2O)_4]^1$	-48.95	-52.07	-42.18
		$[Al(Ser)_{tCNO}(H_2O)_3]^1$	-83.06	-93.73	-83.84
$Al^{3+} - PSer$	NH_3^+, $OHPO_3^-$	$[Al(PSer)_{mC}(H_2O)_5]^2$	-47.98	-40.65	-38.44
		$[Al(PSer)_{bC}(H_2O)_4]^2$	-17.96	-20.38	-18.17
		$[Al(PSer)_{mP}(H_2O)_5]^2$	-37.51	-33.31	-31.10
		$[Al(PSer)_{dCP}(H_2O)_4]^2$	-43.16	-44.10	-41.89
	NH_3^+, OPO_3^{-2}	$[Al(PSer)_{mC}(H_2O)_5]^1$ (†)	-90.05	-81.14	-81.14
		$[Al(PSer)_{mP}(H_2O)_5]^1$	-82.91	-75.93	-75.93
		$[Al(PSer)_{bP}(H_2O)_4]^1$	-71.33	-72.05	-72.05
		$[Al(PSer)_{dCP}(H_2O)_4]^1$	-85.44	-85.66	-85.66
		$[Al(PSer)_{tCP}(H_2O)_3]^1$	-70.22	-79.76	-79.76
	NH_2, OPO_3^{-2}	$[Al(PSer)_{mC}(H_2O)_5]$	-48.16	-43.57	-40.22
		$[Al(PSer)_{N}(H_2O)_5]$ (‡)	-91.15	-82.20	-78.85
		$[Al(PSer)_{mP}(H_2O)_5]$ (†)	-84.25	-79.36	-76.02
		$[Al(PSer)_{bP}(H_2O)_4]$	-63.77	-66.97	-63.63
		$[Al(PSer)_{dCP}(H_2O)_4]$ (†)	-103.22	-102.74	-99.39
		$[Al(PSer)_{tCP}(H_2O)_3]$	-77.92	-87.36	-84.02
		$[Al(PSer)_{tCNP}(H_2O)_3]$	-75.02	-82.53	-79.18
		$[Al(PSer)_{tCNbP}(H_2O)_2]$	-69.76	-86.20	-82.85

dCP, in $[Al\text{-}PSer]^{+1}$, which forms an 8-membered ring, also shows a similar complexation free energy, −85.66 kcal/mol (Fig. 4e). Thus, the binding motifs can be classified in the next decreasing complexation free energy order: dicoordinate binding of carboxylate and phosphate groups with a proton transfer, dCP > tricoordinate binding of carboxylate monodentately and phosphate bidentately, tCP > tetracoordination of the three functional groups with the phosphate in a bidentate mode, tCNbP > dicoordinate binding of carboxylate and phosphate, dCP ≥ tricoordination of the three functional groups, tCNP > monodentate binding of phosphate, mP > bidentate binding of phosphate, bP > monodentate binding of carboxylate, mC > bidentate binding of carboxylate, bC.

The largest complexation free energy of both Al^{3+}-Ser/PSer complexes is obtained for the dCP binding motif in $[Al\text{-}PSer]^0$ complex, −102.74 kcal/mol. Although in general, $[Al\text{-}Ser]^{+1}$ complexes present a bit larger complexation free energies than Al-PSer compounds (a maximum of ~ 6 kcal/mol between the two complexes without any proton transfer and higher complexation free energies), at physiological pH the trend is reversed and $[Al\text{-}Ser]^{+1}$ species competes with $[Al\text{-}PSer]^0$ and $[Al\text{-}PSer]^{1+}$ complexes (see Table 2 and SI). Al-Ser's tCNO and dCO binding modes (−83.84 kcal/mol and −79.05 kcal/mol) competes with Al-PSer's dicoordinate, tricoordinate and tetracoordinate chelated systems (dCP −85.66 kcal/mol, tCP −84.02 kcal/mol, tCNP −79.18 kcal/mol and tCNbP −82.85 kcal/mol). On the other hand, the aluminum binding by phosphate is favored against the alkoxide binding by 4 kcal/mol in +1 charge complexes, ΔG_{aq}^{Phys}= −75.93 kcal/mol vs −71.91 kcal/mol.

The Quantum Theory of " Atoms in Molecules "(QTAIM) is applied to some representative structures of Al-Ser and Al-PSer complexes, see Table 3. As expected, a strong interaction between the aluminum and its coordination sphere is being observed, see Supporting Information. It is well demonstrated in various studies that a strong interaction is connected with a high $\rho(r_{BCP})$ value [57]. In addition, one can observe that Ser and PSer coordination with aluminum presents a positive Laplacian of electron density at Al...O/N BCP, $\nabla^2\rho(r_{BCP})$, indicator of an electrostatic interaction. However, according to $H(r_{BCP})$ there are sizable differences in the bonds obtained for same class interactions in Al-Ser complexes. Thus, the carboxylate and alkoxide interactions with aluminum present a full ionic character in some complexes, with positive values of $H(r_{BCP})$, while they have a small degree of covalancy character in others (small but negative value of $H(r_{BCP})$), see Table 3. Besides, the interaction between the functional groups of PSer and aluminum always presents a small degree of covalency. According to delocalization indexes (DI), the covalency character of the functional groups can be classified in the following decreasing order: alkoxide > phosphate > carboxylate > amine > water (see Fig. 5A). In the case of phosphate interaction, the strength of Al−O bonds depends on the charge of the phosphate and type of coordination mode, with dianionic

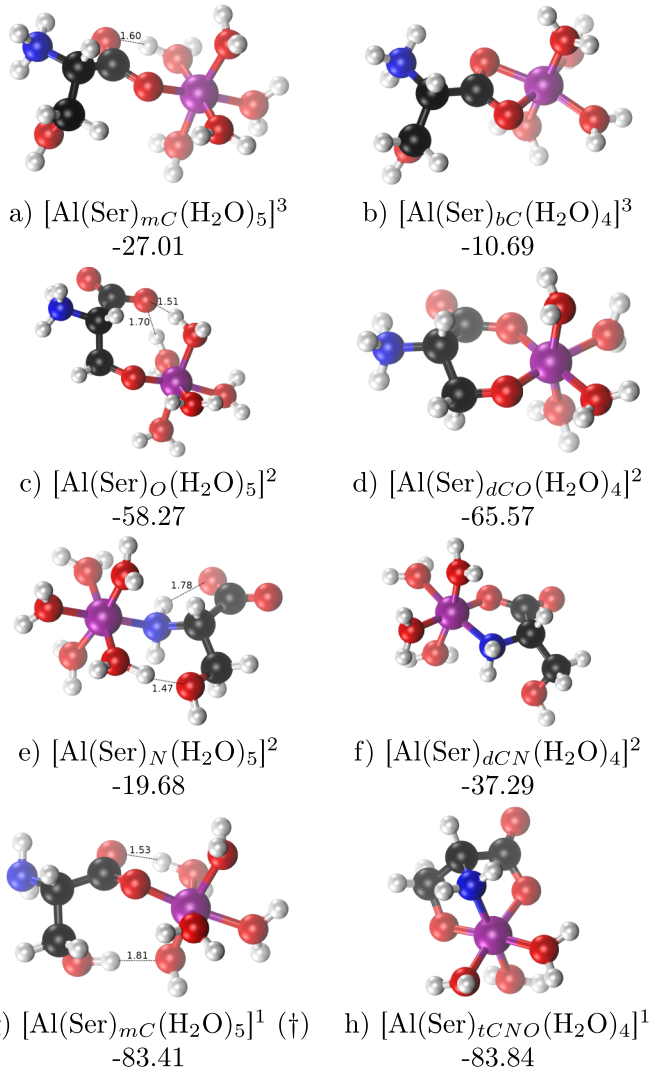

Fig. 3. Representative structures of Al^{3+} − *Ser* complexes. The complexation free energies for the physiological pH (ΔG_{aq}^{Phys}) are shown in kcal/mol. The subscripts indicate the coordination mode of Ser to Al^{3+}: *mC*, monodentate binding of carboxylate; *bC*, bidentate binding of carboxylate; *O*, monodentate binding of alkoxide group; *N* monodentate binding of amine group; *dCO* dicoordinate binding of carboxylate and alkoxide groups; *dCN* dicoordinate binding of carboxylate and amine groups; *tCNO* tricoordinate binding of carboxylate, amine and alkoxide groups. The † sign indicates a spontaneous proton transfer from a water molecule to alkoxide group during the optimization.

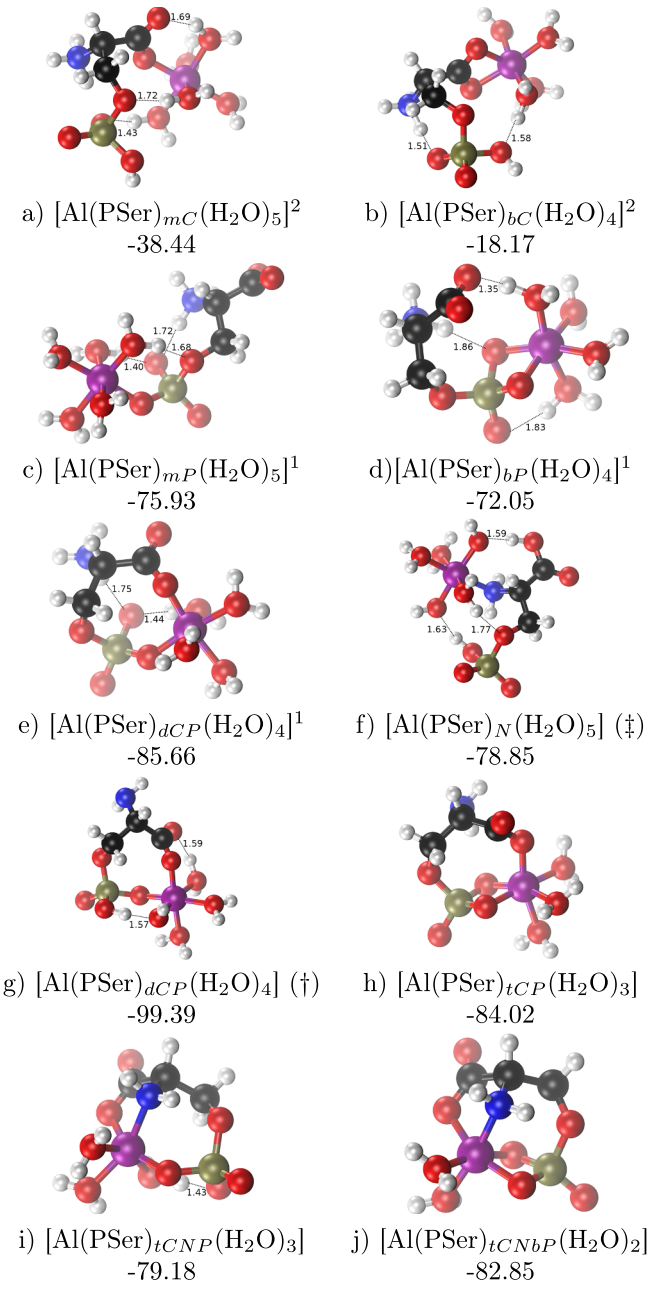

Fig. 4. Representative structures of Al^{3+} − *PSer* complexes. The complexation free energies for the physiological pH (ΔG_{aq}^{Phys}) are shown in kcal/mol. The subscripts indicate the coordination mode of PSer to Al^{3+}: *mC*, monodentate binding of carboxylate; *bC*, bidentate binding of carboxylate; *mP*, monodentate binding of phosphate group; *bP*, bidentate binding of phosphate group; *N* monodentate binding of amine group; *dCP* dicoordinate binding of carboxylate and phosphate groups; *tCNP* tricoordinate binding of carboxylate, amine and phosphate groups; *tCP* tricoordinate binding of carboxylate monodentately and phosphate bidentately; *tCNbP* tetracoordinate binding of carboxylate and amine groups monodentately and phosphate group bidentately. The † sign indicates a spontaneous proton transfer from a water molecule to phosphate group during the optimization. While the ‡ sign indicates two spontaneous proton transfer from a water molecule to the phosphate group and from another water molecule to carboxylate group during the optimization.

monodentade phosphate groups showing the largest DI's (see Fig. 5B). On the other hand, aluminum first solvation water molecules have a tendency to make strong hydrogen bonds with other oxygen atoms in Al-PSer complexes. They present high values of $\rho(r_{BCP})$ (in the range of 0.0334 –0.0894 au) in comparison with typical hydrogen bonds, see Supporting Information. Moreover, most of these hydrogen bonds, *H...O*, show a negative $H(r_{BCP})$, which can be treated as the covalency of *H...O* interaction. One can see that the covalent character increases for shorter hydrogen bond distances, see Supporting Information.

3.2. $[Al(OH)]^{2+}$ species

In this section, one water molecule of the coordination sphere of Al^{3+} is ionized to give $[Al(OH)(H_2O)_5]^2$. Therefore, we analyze the energetics corresponding to the complexation of Ser and PSer with $[Al(OH)]^{2+}$ by the different functional groups of each species (see Fig. 2B).

We have considered 19 $[Al(OH)]^{2+}$ − *Ser* complexes that differ in coordination mode and protonation states of Ser (see Supporting Information). The resultant charges of the complexes are +2, +1 and 0. We find that there is an increase in binding affinity with the reduction of the positive charge of the complex, obtaining the largest complexation free energy for the neutral charged compounds (see Fig. 2B

Table 3
Distance (in Å) and electron delocalization indexes (DI) of aluminum interactions with the functional groups in representative Al^{3+}-Ser/PSer structures. QTAIM parameters of *Al…O* and *Al…N* bond critical points (BCP, in au): $\rho(r_{BCP})$, the electron density at BCP; $\nabla^2\rho(r_{BCP})$, the Laplacian of the electron density; and $H(r_{BCP})$, the total electron energy density at BCP. O_C stands for carboxylate group oxygen atom, O_P for phosphate group oxygen atom, *O* for alkoxide oxygen atom, and O_W for average water oxygen.

Titratable groups	Structure	Distance		DI	$\rho(r_{BCP})$	$\nabla^2\rho(r_{BCP})$	$H(r_{BCP})$
NH_3^+, O^-	$[Al(Ser)_{dCO}(H_2O)_4]^2$	Al-O_C	1.844	0.180	0.0697	0.5118	0.0063
		Al-O	1.779	0.226	0.0854	0.6698	0.0053
		Al-O_W	1.970	0.123	0.0486	0.3134	0.0045
	$[Al(Ser)_{O}(H_2O)_5]^2$	Al-O	1.768	0.220	0.0843	0.6847	0.0076
		Al-O_W	1.946	0.134	0.0523	0.3437	0.0046
NH_2, O^-	$[Al(Ser)_{dCO}(H_2O)_4]^1$	Al-O_C	1.827	0.198	0.0787	0.5040	-0.0030
		Al-O	1.766	0.245	0.0951	0.6240	-0.0091
		Al-O_W	1.983	0.124	0.0502	0.2964	0.0016
	$[Al(Ser)_{dCN}(H_2O)_4]^1$	Al-O_C	1.811	0.208	0.0794	0.5939	0.0046
		Al-N	2.000	0.176	0.0620	0.3189	-0.0045
		Al-O_W	1.949	0.133	0.0513	0.3395	0.0051
	$[Al(Ser)_{tCNO}(H_2O)_3]^1$	Al-O_C	1.880	0.181	0.0717	0.4193	-0.0042
		Al-O	1.803	0.226	0.0882	0.5496	-0.0084
		Al-N	2.048	0.151	0.0569	0.2471	-0.0076
		Al-O_W	1.960	0.135	0.0531	0.3172	0.0016
NH_3^+, $OHPO_3^-$	$[Al(PSer)_{mC}(H_2O)_5]^2$	Al-O_C	1.844	0.178	0.0737	0.4691	-0.0017
		Al-O_W	1.922	0.149	0.0599	0.3631	0.0005
	$[Al(PSer)_{dCP}(H_2O)_4]^2$	Al-O_C	1.865	0.169	0.0690	0.4352	-0.0008
		Al-O_P	1.823	0.189	0.0762	0.5068	-0.0010
		Al-O_W	1.943	0.140	0.0565	0.3363	0.0007
NH_3^+, OPO_3^{-2}	$[Al(PSer)_{dCP}(H_2O)_4]^1$	Al-O_C	1.843	0.176	0.0714	0.4691	-0.0001
		Al-O_P	1.815	0.204	0.0804	0.5220	-0.0034
		Al-O_W	1.959	0.136	0.0546	0.3198	0.0006
NH_2, OPO_3^{-2}	$[Al(PSer)_{tCP}(H_2O)_3]$	Al-O_C	1.825	0.190	0.0763	0.5026	-0.0015
		Al-O_P	1.875	0.188	0.0727	0.4299	-0.0050
		Al-O_P	1.888	0.181	0.0702	0.4121	-0.0045
		Al-O_W	1.981	0.127	0.0508	0.2973	0.0012
	$[Al(PSer)_{tCNP}(H_2O)_3]$	Al-O_C	1.867	0.199	0.0740	0.4368	-0.0047
		Al-O_P	1.803	0.229	0.0845	0.5447	-0.0055
		Al-N	2.116	0.132	0.0499	0.2002	-0.0066
		Al-O_W	2.008	0.126	0.0485	0.2703	0.0004

and Table 4). On the other hand, the mono- and bidentate binding mode of carboxylate group is analyzed in the four possible protonation states of Ser, being the monodentate binding mode favored against the bidentate one by at least 6 kcal/mol depending on the species (see Table 4 and SI). In addition, the monoanionic species with NH_3^+/O^- titratable groups are preferred over NH_2/OH tautomers, despite the larger penalty in the complexation free energies at physiological pH due to the deprotonation of the alcohol group in the first type of compounds (see Table 1). The same was observed for Al^{3+} complexes. Besides, the formation of rings is favored in both tautomeric species by the dicoordinate binding mode of carboxylate and alkoxide/amine groups (see SI). As a matter of fact, it should be mentioned that the coordination of $[Al(OH)]^{2+}$ by alkoxide presents a higher complexation free energy than the dicoordinate binding by carboxylate and amine groups, dCN, by around 10 kcal/mol (ΔG_{aq}^{Phys}= −40.90 kcal/mol vs −30.27 kcal/mol in +1 complexes, see Table 4). Finally, the tricoordinate binding mode by the three functional groups, tCNO, which forms (6+5+5)-membered joint rings, is the preferred coordination mode in [Al-Ser]^0 complexes, ΔG_{aq}^{compl}= −77.13 kcal/mol, followed by the dicoordinate binding mode of carboxylate and alkoxide groups (dCO, ΔG_{aq}^{compl}= −70.53 kcal/mol). Therefore, the binding motifs can be sorted in the next decreasing complexation free energy order: tCNO > dCO > O > dCN > mC > bC > N.

On the other hand, a total of 29 $[Al(OH)]^{2+}$ − *PSer* complexes are analyzed with total charges of +1, 0 and −1(see Fig. 2B and SI). The smallest complexation free energies are obtained for +1 complexes, while the highest ones are obtained for −1 charge systems. Thus, the charge is a driving factor for the binding affinity. In addition, monodentate binding mode to carboxylate group is preferred against the bidentate one (ΔG_{aq}^{compl}= −25.27 kcal/mol vs −9.96 kcal/mol), while the opposite is observed for the phosphate group (bidentate binding mode is favored), −59.97 kcal/mol vs −54.93 kcal/mol, see Table 4 and SI.

The dicoordinate binding mode of aluminum by carboxylate and phosphate groups, dCP, where an 8-membered ring is formed, presents the highest complexation free energy in the three different types of complexes (see Table 4). Besides, the formation of joint rings is favored against the monodentate binding mode (see SI). Therefore, tCP and tCNbP binding motifs show also a high complexation free energy. Surprisingly, the tricoordinate chelation of $[Al(OH)]^{2+}$ by the three functional groups, tCNP, presents a smaller complexation free energy than the bidentate binding of phosphate group, −47.80 kcal/mol vs −52.48 kcal/mol. Thus, the binding modes can be organized in the next decreasing complexation free energy order: dCP > tCNbP > tCP > bP > tCNP > mP > mC > bC.

The largest complexation free energy at physiological pH of $[Al(OH)]^{2+}$-Ser/PSer complexes is obtained for the dCP binding motif in [Al-PSer]$^{-1}$ complex, −71.69 kcal/mol. Al-PSer compounds present larger complexation free energies at physiological pH than Al-Ser complexes, although the preferred binding motif in Al-Ser species,

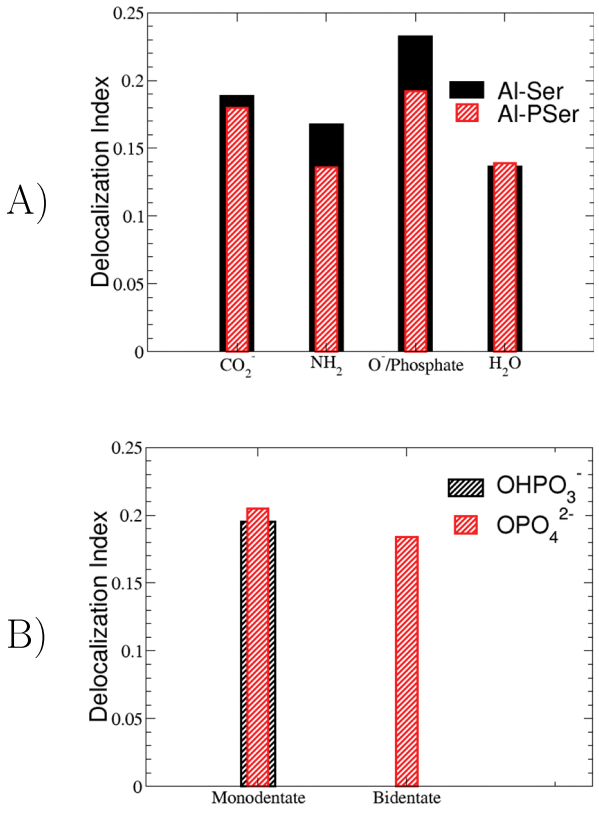

Fig. 5. Average delocalization indexes. A) Average for each functional group in Al^{3+} − *Ser/PSer* structures. B) Average for phosphate group in monoanionic (black) and dianionic (red) Al^{3+} − *PSer* complexes.

tCNO in [Al-Ser]^0, is only 4 kcal/mol behind, ΔG_{aq}^{Phys}= −67.24 kcal/mol. Moreover, the aluminum binding by phosphate is favored against the alkoxide binding by 7 kcal/mol in neutral complexes (−54.93 kcal/mol vS −47.27 kcal/mol, see Table 4 and SI).

The application of the QTAIM theory to some representative structures of Al-Ser and Al-PSer complexes are shown in Supporting Information. Similar features are observed for the Al—O and Al—N bonds in $[Al(OH)]^{2+}$ species to the ones previously mentioned in the case of Al^{3+} compounds. According to DI's the strongest interaction corresponds to the aluminum-hydroxide interaction with the following decreasing order in DI's: hydroxide > alkoxide > phosphate > carboxylate > amine > water. It is worthwhile to highlight, that the presence of a hydroxide in the first coordination shell of aluminum has a sizable and weakening effect on the strength of the rest of the aluminum-ligand interactions. For instance, in the case of [Al(PSer)$_{tCNP}$(H$_2$O)$_3$] the DI's for the different aluminum-ligand bonds are 0.229 ($Al-O_P$) > 0.199 ($Al-O_C$) > 0.132 ($Al-N$) > 0.126 ($Al-O_W$), whereas for [Al(PSer)$_{tCNP}$(H$_2$O)$_2$(OH)]$^-$ the figures are 0.228 ($Al-O_H$) > 0.203 ($Al-O_P$) > 0.170 ($Al-O_C$) > 0.129 ($Al-N$) > 0.115 ($Al-O_W$). This lowering in DI's by the presence of a hydroxide is consistent with the lower binding affinities observed in the case of $[Al(OH)]^{2+}$ species with respect to Al^{3+} compounds.

3.3. $[Al(OH)_2]^+$ species

In this section, two water molecules of the coordination sphere of aluminum are hydrolyzed to give [Al(OH)$_2$(H$_2$O)$_4$]^1($[Al(OH)_2]^+$ hereafter). Therefore, we analyze the energetics corresponding to the complexation of $[Al(OH)_2]^+$ with Ser and PSer by the different functional groups of each species.

We have considered 17 Al-Ser complexes that differ in coordination mode and ionic species of Ser, see Supporting Information. The resultant charge of the complexes are +1, 0 and −1. We find that there is an increase in binding affinity with the reduction of the charge of the complex, obtaining the largest complexation free energy for the monoanionic compounds (see Fig. 2C and Table 5). On the other hand, the mono- and bidentate binding mode of carboxylate group is analyzed in the four possible ionic species of Ser, the monodentate binding mode being favored in the neutral and positively charge complexes by at least 4 kcal/mol, while the bidentate binding is favored by 2 kcal/mol in the anionic complexes (see Table 5 and SI).

In addition, the neutral species with $-NH_3^+$ and $-O^-$ titratable groups are preferred against their tautomers with $-NH_2$ and −OH titrable groups, despite the larger penalty in the complexation free energy at physiological pH due to the deprotonation of the alcohol group in the first type of compounds (see Table 1). As a matter of fact, the same was observed for Al^{3+} and $[Al(OH)]^{2+}$ complexes. Besides, the formation of rings is favored in both ionic species by dCO and dCN binding motifs. Moreover, it should be mentioned that the coordination of $[Al(OH)_2]^+$ by alkoxide presents a higher complexation free energy than the dicoordinate binding by carboxylate and amine groups by around 6 kcal/mol, although the difference is reduced to less than 1 kcal/mol at the physiological pH (see Table 5 and SI).

Finally, the tricoordinate chelation by the three functional groups, tCNO, which forms (6+5+5)-membered joint rings, is the preferred coordination mode in Al-Ser^{-1} complexes, ΔG_{aq}^{compl}= −55.01 kcal/mol, followed by the dicoordinate binding mode of carboxylate and alkoxide groups (dCO, ΔG_{aq}^{compl}= −47.87 kcal/mol). Therefore, the binding motifs can be sorted in the next decreasing complexation free energy order: tCNO > dCO > O > dCN > mC > bC > N.

On the other hand, a total of 20 Al-PSer complexes are analyzed with total charges of 0, −1 and −2(see Fig. 2C and SI). The smallest complexation free energies are obtained for +1 complexes, while the highest ones are obtained for −1 charge systems, although at physiological pH the monoanionic and dianionic complexes present very similar ΔG_{aq}^{Phys} (see Table 5). This behavior is indicative that we are reaching the saturation limit of negative charge coordination to the metal positive center.

In addition, the formation of chelated systems is preferred against the monodentate complexes. The bidentate binding mode of phosphate group is favored against the monodentate one. Moreover, the dicoordinate binding of aluminum by carboxylate and phosphate groups, dCP, where an 8-membered ring is formed, shows the highest complexation free energy (see Table 5 and SI).

The binding motifs can be classified in the next decreasing complexation free energy order: dCP > tCP > bP > mP > N > mC > bC.

The largest complexation free energy at physiological pH of $[Al(OH)_2]^+$-Ser/PSer species is obtained for the tCNO binding motif in [Al-Ser]$^{-1}$ complex, −45.12 kcal/mol, followed from very closely by [Al-PSer]$^{-1}$ dCP (−43.85 kcal/mol), tCP (−42.10 kcal/mol) and bP (−42.22 kcal/mol) binding motifs. In general, Al-PSer compounds present larger complexation free energies at physiological pH than Al-Ser complexes (see SI). Moreover, the aluminum binding by phosphate is favored against the alkoxide binding by 11 kcal/mol in monoanionic complexes (−41.62 kcal/mol vS −30.51 kcal/mol, see Table 5).

The application of the QTAIM theory to some representative structures of Al-Ser and Al-PSer complexes are shown in the Supporting Information. The order in DI's is similar to the one commented before for $[Al(OH)_2]^{2+}$ compounds with hydroxide > alkoxide > phosphate > carboxylate > amine > water. The presence of a second hydroxide has a further weakening effect on the rest of aluminum-ligand interactions, consistent with the lowest binding affinities for $[Al(OH)_2]^+$ species.

3.4. Discussion

Our calculations show a variety of possible competitive structures for aluminum binding, which lead to a rich diversity of potential

Table 4
Enthalpy and free energy affinities in kcal/mol for $[Al(OH)]^{2+} - Ser/PSer$ complexes formation with corrections that account for the physiological pH and de/protonation of the corresponding titratable groups. The subscripts indicate the coordination mode of Ser/PSer to $[Al(OH)]^{2+}$. The † sign indicates a spontaneous proton transfer from a water molecule to phosphate group during the geometry optimization.

	Titratable groups	Structure	ΔH_{aq}^{compl}	ΔG_{aq}^{compl}	ΔG_{aq}^{Phys}
$[Al(OH)]^{2+} - Ser$	NH_3^+, OH	$[Al(Ser)_{mC}(H_2O)_4(OH)]^2$	-19.67	-15.34	-15.34
		$[Al(Ser)_{bC}(H_2O)_3(OH)]^2$	-2.95	-5.99	-5.99
	NH_3^+, O^-	$[Al(Ser)_{bC}(H_2O)_3(OH)]^1$	-12.04	-14.59	-6.95
		$[Al(Ser)_{O}(H_2O)_4(OH)]^1$	-54.79	-48.54	-40.90
		$[Al(Ser)_{dCO}(H_2O)_3(OH)]^1$	-55.91	-58.27	-50.63
	NH_2, OH	$[Al(Ser)_{mC}(H_2O)_4(OH)]^1$	-34.14	-27.90	-25.65
		$[Al(Ser)_{bC}(H_2O)_3(OH)]^1$	-17.20	-19.65	-17.40
		$[Al(Ser)_{N}(H_2O)_4(OH)]^1$	-23.47	-16.99	-14.74
		$[Al(Ser)_{dCN}(H_2O)_3(OH)]^1$	-29.95	-32.53	-30.27
	NH_2, O^-	$[Al(Ser)_{mC}(H_2O)_4(OH)]$	-42.97	-37.09	-27.20
		$[Al(Ser)_{bC}(H_2O)_3(OH)]$	-27.68	-30.92	-21.03
		$[Al(Ser)_{O}(H_2O)_4(OH)]$	-64.69	-57.16	-47.27
		$[Al(Ser)_{dCO}(H_2O)_3(OH)]$	-68.21	-70.53	-60.64
		$[Al(Ser)_{dCN}(H_2O)_3(OH)]$	-39.14	-40.20	-30.30
		$[Al(Ser)_{tCNO}(H_2O)_2(OH)]$	-68.37	-77.13	-67.24
$[Al(OH)]^{2+} - PSer$	NH_3^+, $OHPO_3^-$	$[Al(PSer)_{mC}(H_2O)_4(OH)]^1$	-36.20	-25.27	-23.06
		$[Al(PSer)_{bC}(H_2O)_3(OH)]^1$	-9.30	-9.96	-7.75
		$[Al(PSer)_{mP}(H_2O)_4(OH)]^1$	-24.34	-18.85	-16.64
		$[Al(PSer)_{dCP}(H_2O)_3(OH)]^1$	-30.03	-29.74	-27.53
	NH_3^+, OPO_3^{-2}	$[Al(PSer)_{mC}(H_2O)_4(OH)]$ (†)	-64.63	-54.76	-54.76
		$[Al(PSer)_{mP}(H_2O)_4(OH)]$	-62.73	-54.93	-54.93
		$[Al(PSer)_{bP}(H_2O)_3(OH)]$	-59.88	-59.97	-59.97
		$[Al(PSer)_{dCP}(H_2O)_3(OH)]$	-69.06	-65.98	-65.98
		$[Al(PSer)_{tCP}(H_2O)_2(OH)]$	-54.69	-62.06	-62.06
	NH_2, OPO_3^{-2}	$[Al(PSer)_{mC}(H_2O)_4(OH)]^-$	-30.76	-25.57	-22.23
		$[Al(PSer)_{bP}(H_2O)_3(OH)]^-$	-51.73	-52.48	-49.14
		$[Al(PSer)_{N}(H_2O)_4(OH)]^-$	-44.35	-34.00	-30.66
		$[Al(PSer)_{dCP}(H_2O)_3(OH)]^-$	-78.49	-75.04	-71.69
		$[Al(PSer)_{tCP}(H_2O)_2(OH)]^-$	-58.34	-65.61	-62.27
		$[Al(PSer)_{tCNP}(H_2O)_2(OH)]^-$	-42.24	-47.80	-44.46
		$[Al(PSer)_{tCNbP}(H_2O)(OH)]^-$	-52.36	-67.01	-63.67

structures to be formed. Our results show that the phosphorylation of serine increases its affinity for aluminum. As a summary of the most stable structures we show the ΔG_{aq}^{comp} and ΔG_{aq}^{Phys} (see Fig. 6) versus the sum of delocalization indexes in $Al - X$ bonds ($X = O, N$) for the six most stable structures in each hydrolytic species for Al-Ser and Al-PSer compounds. It is clear from the figure that in both families of compounds the complexation free energies decrease in the following order $Al^{3+} > [Al(OH)]^{2+} > [Al(OH)_2]^+$, which is in agreement with the known higher ability of aluminum to bind polypeptides as the pH lowers [27].

On the other hand, the introduction of a phosphate group in the peptide increases the binding ability of the peptide towards aluminum, specially if we consider $\triangle G_{aq}^{Phys}$ values. Thus, upon deprotonation of the alkoxide a very strong Al−O bond is created with high values of delocalization index and high values of ΔG_{aq}^{comp} (Al^{3+}, 0.245 au and −81.8 kcal/mol, respectively). In fact, some of these Al-Ser structures show consistently higher ΔG_{aq}^{comp} than some of the Al-PSer species (especially those that do not imply a proton transfer from the surrounding water molecules to the phosphate). However, when $\triangle G_{aq}^{Phys}$ are considered, and therefore, the energy penalty to deprotonate the alcohol is taken into account, the higher affinity of aluminum to PSer is clearly evidenced for all the hydrolytic species. In particular, the next is observed:

Al^{3+}: The preferred ligand is PSer by at least ∼ 9 kcal/mol. Nevertheless, if we do not take into account the most stable structure, $[Al(PSer)_{dCP}(H_2O)_4]$, where a proton transfer from a surrounding water molecule to the phosphate was observed during optimization, $[Al(Ser)_{tCNO}(H_2O)_3]^1$ is ∼ 6 kcal/mol higher in ΔG_{aq}^{comp} than $[Al(PSer)_{tCP}(H_2O)_3]$. However, at physiological pH this trend is reversed and PSer is the preferred ligand by ∼ 2 kcal/mol (−83.84 vs −85.66 kcal/mol).

$[Al(OH)]^{2+}$: $[Al(Ser)_{tCNO}(H_2O)_2(OH)]$ is ∼ 2 kcal/mol higher in ΔG_{aq}^{comp} than $[Al(PSer)_{dCP}(H_2O)_3(OH)]^-$. However, at physiological pH the trend is reversed and PSer is the preferred ligand by ∼ 4.5 kcal/mol (−67.24 vs −71.69 kcal/mol).

$[Al(OH)_2]^+$: $[Al(Ser)_{tCNO}(H_2O)(OH)_2]^-$ is ∼ 8 kcal/mol higher in ΔG_{aq}^{comp} than $[Al(PSer)_{dCP}(H_2O)_2(OH)_2]^{-2}$. However, at physiological pH this difference is significantly reduced to ∼ 1 kcal/mol (−45.12 vs −43.83 kcal/mol).

With respect to the preferred chelated motif, there are substantial changes depending on the hydrolytic species and whether the peptide is phosphorylated or not (see Fig. S1 in SI). The preferred binding motif in Al-Ser complexes by at least 4 kcal/mol is the tricoordination binding of aluminum by the three titratable groups, tCNO (carboxilate, amine and alkoxide), followed by the dicoordinate binding by carboxylate and alkoxide groups, dCO. While for the Al-PSer complexes, the preferred binding pattern is the dicoordinate binding by carboxylate and phosphate groups, dCP. Although, the tricoordinate and tetracoordinate chelations, tCP and tCNbP, present just a bit lower free energies, followed by the monodentate coordination of the phosphate group. All these binding motifs lie very close in energy. It should be also mentioned, that the phosphate group shows a small preference for the monodentate coordination of Al^{3+}, while for $[Al(OH)]^{2+}$ and $[Al(OH)_2]^+$ it seems to prefer the bidentate coordination. A previous experimental work of Kiss et al. [40] suggests that in Al-PSer complexes aluminum was coordinated monodentately by phosphate group or

Table 5
Enthalpy and free energy affinities in kcal/mol for $[Al(OH)_2]^{1+} - Ser/PSer$ complexes formation with corrections that account for the physiological pH and de/protonation of the corresponding titratable groups. The subscripts indicate the coordination mode of Ser/PSer to $[Al(OH)_2]^{1+}$.

	Titratable groups	Structure	ΔH_{aq}^{compl}	ΔG_{aq}^{compl}	ΔG_{aq}^{Phys}
$[Al(OH)_2]^+ - Ser$	NH_3^+, OH	$[Al(Ser)_{mC}(H_2O)_3(OH)_2]^1$	-10.64	-6.74	-6.74
		$[Al(Ser)_{bC}(H_2O)_2(OH)_2]^1$	0.28	-2.98	-2.98
	NH_3^+, O^-	$[Al(Ser)_{mC}(H_2O)_3(OH)_2]$	-22.94	-16.09	-8.44
		$[Al(Ser)_{bC}(H_2O)_2(OH)_2]$	-6.28	-9.51	-1.87
		$[Al(Ser)_{O}(H_2O)_3(OH)_2]$	-33.80	-28.68	-21.04
		$[Al(Ser)_{dCO}(H_2O)_2(OH)_2]$	-35.20	-37.13	-29.49
	NH_2, OH	$[Al(Ser)_{mC}(H_2O)_3(OH)_2]$	-24.00	-19.36	-17.11
		$[Al(Ser)_{bC}(H_2O)_2(OH)_2]$	-10.89	-14.45	-12.20
		$[Al(Ser)_{N}(H_2O)_3(OH)_2]$	-15.86	-9.82	-7.57
		$[Al(Ser)_{dCN}(H_2O)_2(OH)_2]$	-20.17	-22.96	-20.71
	NH_2, O^-	$[Al(Ser)_{mC}(H_2O)_3(OH)_2]^{-1}$	-22.16	-18.70	-8.81
		$[Al(Ser)_{bC}(H_2O)_2(OH)_2]^{-1}$	-16.68	-20.79	-10.89
		$[Al(Ser)_{O}(H_2O)_3(OH)_2]^{-1}$	-46.70	-40.40	-30.51
		$[Al(Ser)_{dCO}(H_2O)_2(OH)_2]^{-1}$	-44.99	-47.87	-37.97
		$[Al(Ser)_{dCN}(H_2O)_2(OH)_2]^{-1}$	-26.09	-28.79	-18.90
		$[Al(Ser)_{tCNO}(H_2O)(OH)_2]^{-1}$	-45.74	-55.01	-45.12
$[Al(OH)_2]^+ - PSer$	NH_3^+, $OHPO_3^-$	$[Al(PSer)_{mC}(H_2O)_3(OH)_2]$	-24.46	-15.37	-13.16
		$[Al(PSer)_{bC}(H_2O)_2(OH)_2]$	-2.78	-6.01	-3.80
		$[Al(PSer)_{mP}(H_2O)_3(OH)_2]$	-14.26	-9.00	-6.79
		$[Al(PSer)_{dCP}(H_2O)_2(OH)_2]$	-13.26	-13.80	-11.59
	NH_3^+, OPO_3^{-2}	$[Al(PSer)_{mC}(H_2O)_3(OH)_2]^{-1}$	-21.24	-13.31	-13.31
		$[Al(PSer)_{mP}(H_2O)_3(OH)_2]^{-1}$	-49.09	-41.62	-41.62
		$[Al(PSer)_{bP}(H_2O)_2(OH)_2]^{-1}$	-41.91	-42.22	-42.22
		$[Al(PSer)_{dCP}(H_2O)_2(OH)_2]^{-1}$	-46.04	-43.85	-43.85
		$[Al(PSer)_{tCP}(H_2O)(OH)_2]^{-1}$	-35.47	-42.10	-42.10
	NH_2, OPO_3^{-2}	$[Al(PSer)_{mC}(H_2O)_3(OH)_2]^{-2}$	-30.79	-22.02	-18.67
		$[Al(PSer)_{mP}(H_2O)_3(OH)_2]^{-2}$	-35.46	-27.53	-24.19
		$[Al(PSer)_{bP}(H_2O)_2(OH)_2]^{-2}$	-32.34	-34.71	-31.37
		$[Al(PSer)_{N}(H_2O)_3(OH)_2]^{-2}$	-35.07	-26.61	-23.27
		$[Al(PSer)_{dCP}(H_2O)_2(OH)_2]^{-2}$	-50.85	-47.18	-43.83
		$[Al(PSer)_{tCP}(H_2O)(OH)_2]^{-2}$	-32.77	-39.70	-36.36

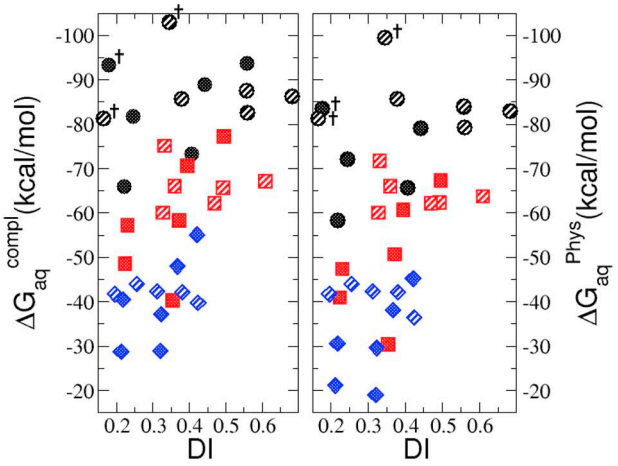

Fig. 6. Complexation (ΔG_{aq}^{comp}, left) and physiological (ΔG_{aq}^{Phys}, right) free energies and delocalization indexes for Al-Ser (filled symbols) and Al-PSer (striped symbols) complexes: black circles Al^{3+} species; red squares $[Al(OH)]^{2+}$ compounds; and blue diamonds $[Al(OH)_2]^+$ structures. The † sign indicates a spontaneous proton transfer from a water molecule to alkoxide/phosphate group during the optimization.

chelated in a tridentate fashion by the three titratable groups, tCNP. Regarding our results, we think that the tricoordinate binding pattern, where a joint ring structure is formed, is more favorable than the monodentate one.

As we have commented above, there is a decrease in the affinity of both Ser and PSer to aluminum as we increased the number of hydroxides in the first coordinaton shell around aluminum. This is also mirrored in lower DI's. Thus, the presence of hydroxides tends to lower the ability of aluminum to establish strong Al—O interactions with peptides. At neutral pH, aluminum is chelated by four hydroxide molecules. Could this hydrolytic species still have a favorable interaction with Ser or PSer? To analyze this possibility we have calculated the complexation free energy of displacement of one of the hydroxides of the first solvation layer of $[Al(OH)_4]^-$ by Ser's in two protonation states, *SerOH* and $SerO^-$, and *PSer* with the phosphate group either in the monoanionic ($HPSer^-$) or the dianionic protonation state ($PSer^{2-}$). Results are summarized in Table 6. We remind that according to the experimental pKa's of alcohols and phosphates, the most likely protonation states are *SerOH* and $PSer^{2-}$ at physiological pH. Two types of reactions can be found in Table 6. Those reactions in which a negatively charged functional group, $SerO^-/HPSer^-/PSer^{2-}$, displaces a hydroxide ligand from the first coordination layer around aluminum, and those reactions in which the hydroxide displacement is accompanied by a proton transfer to the hydroxide from the protonated *SerOH*/$HPSer^-$ groups. According to our results, the displacement of a hydroxide departing from an already deprotonated Ser/Pser is only favorable in the case of dianionic $PSer^{-2}$ with the following order in preference $PSer^{2-} > SerO^- > HPSer^-$. It is interesting to note that once deprotonated and for compounds of the same charge $SerO^-$ has a stronger interaction than $HPSer^-$. Nevertheless, our results suggest that the strong interaction of Al(III) with hydroxide precludes in general the interaction of aluminum with ligands of equal charge such as $SerO^-$/$HPSer^-$. Delocalization indexes follow these trends, and they decrease in the following order $OH > SerO^- > HPSer^-$.

However, when we depart from protonated $SerOH/HPSer^{-1}$ and consider reactions in which the hydroxide substitution is coupled with proton transfer, now the attack of $HPSer^-$ is more favorable and exothermic, −5.89 kcal/mol, than the attack of *SerOH*, 4.36 kcal/mol. Two

Table 6
Delocalization indexes, enthalpy and free energy affinities in kcal/mol for $[Al(OH)_4]^- - Ser/PSer$ complexes formation with corrections that account for the physiological pH and de/protonation of the corresponding titratable groups. The subscripts indicate the coordination mode of Ser/PSer to $[Al(OH)_4]^-$. O_C stands for carboxylate group oxygen atom, O_P for phosphate group oxygen atom and O_H for average hydroxy group oxygen atom. $\Delta G_{aq}^{Phys}(pOH)$ takes into account the entropic factor that accounts for the hydroxide concentration at physiological pH ($\Delta G_{aq}^{Phys}(pOH) = \Delta G_{aq}^{Phys} - n_{OH}(14 - pH)RTln10$).

	Titratable groups	Structure	ΔH_{aq}^{compl}	ΔG_{aq}^{compl}	ΔG_{aq}^{Phys}	ΔG_{aq}^{Phys}(pOH)	DI	
$[Al(OH)_4]^- + SerOH \rightarrow [Al(OH)_3Ser]^- + H_2O$	NH_3^+, OH	$[Al(Ser)_O(OH)_3]^{-1}$	−0.97	4.36	4.36	4.36	$Al - O_C$	0.237
							$Al - O_H$	0.265
$[Al(OH)_4]^- + SerO^- \rightarrow [Al(OH)_3Ser]^- + OH^-$	NH_3^+, O^-		1.63	5.93	13.58	4.57		
$[Al(OH)_4]^- + HPSer^- \rightarrow [Al(OH)_3HPSer]^- + OH^-$	NH_3^+, $OHPO_3^-$	$[Al(PSer)_{mP}(OH)_3]^{-1}$	17.68	22.05	24.26	15.26	$Al - O_P$	0.203
							$Al - O_H$	0.274
$[Al(OH)_4]^- + HPSer^- \rightarrow [Al(OH)_3PSer]^{-2} + H_2O$	NH_3^+, $OHPO_3^-$	$[Al(PSer)_{mP}(OH)_3]^{-2}$	−15.00	−8.10	−5.89	−5.89	$Al - O_P$	0.229
$[Al(OH)_4]^- + PSer^{2-} \rightarrow [Al(OH)_3PSer]^{-2} + OH^-$	NH_3^+, OPO_3^{-2}		−12.32	−5.88	−5.88	−14.88	$Al - O_H$	0.267

important conclusions arise from these data: i) if deprotonation of the attacking group is taken into account, the binding of a monophoshate-serine is significantly more favorable than the attack of the serine, and ii) the protonation of the leaving hydroxide favors the reaction. Overall if we consider the most likely species at physiological pH, *SerOH* and $PSer^{2-}$, we can say that phosphorylation of the serine has a deep effect on the affinity of the peptide towards aluminum. Whereas the displacement of a hydroxide by serine is clearly endothermic, 4.36 kcal/mol, the reaction's free energies for $PSer^{-2}$ are all clearly exothermic, −14.88 kcal/mol. Thus, the phosphorylation of serine can increase the affinity towards aluminum sufficiently as to displace hydroxides from the first coordination layer around aluminum at physiological pH. Notice that DI's of $Al - O_H$ are still higher than the ones for $Al - O_P$ (0.267 vs 0.229 au), but the higher electrostatic interaction with a −2 charged phosphate-monoester compensates for a lower DI, and therefore, a higher electron donation from hydroxide to aluminum. In summary, the enhancement on affinity of PSer over serine arises from two factors: i) the larger negative charge of a $PSer^{2-}$ phosphate group and ii) the deprotonation energy penalty of the *SerOH* group. These two factors combined make phosphorylation of peptide a fundamental factor in the affinity of polypeptides and proteins towards aluminum, and it could be one of the defining structural factors in the interaction of proteins with this exogeneous metal.

4. Conclusions

In this paper we have studied the interaction of different aluminum hydrolytic species with serine and phosphoserine in order to shed light on the aluminum-binding abilities of phosphorylated proteins and peptides. Our calculations confirm the known higher ability of aluminum to bind polypeptides as the pH lowers and show a variety of possible competitive structures for aluminum binding, which lead to a rich diversity of potential structures to be formed. With respect to the preferred chelated motif, both ligands show a tendency to form rings. tCNO is the most favorable binding motif in Al-Ser complexes, forming a structure with (6 + 5 + 5)-membered joint rings, while dCP chelation is the preferential one in Al-PSer complexes, where an 8-membered ring is formed.

Our results show unambiguously that phosphorylation increases the binding capacity of the peptide towards aluminum. This is especially true at physiological pH when an $Al(OH)_4^-$ is taken into account as the reference aluminum hydrolytic species. In this case, the displacement of an hydroxide from aluminum is clearly endothermic in the case of Ser, whereas it is exothermic in the case of PSer. The reason for the higher stability of Al-PSer compounds over Al-Ser ones is a combination of a higher electrostatic interaction with a double negatively charged phosphate monoester compound and the energy penalty associated with the deprotonation of the alcohol group in Serine.

Abbreviations

PSer: Phosphoserine
AD: Alzheimer's disease
NFT: Neurofilament Tangle
DFT: Density Functional Theory
QTAIM: Quantum Theory of "Atoms in Molecules"
BCP: Bond Critical Point
SI: Supporting Information
mC: monodentate binding by carboxylate group
bC: bidentate binding by carboxylate group
O: monodentate binding by alkoxide group
N: monodentate binding by amine group
mP: monodentate binding by phosphate group
bP: bidentate binding by phosphate
dCO: dicoordinate binding by carboxylate and phosphate groups
dCP: dicoordinate binding by carboxylate and phosphate groups
dCN: dicoordinate binding by carboxylate and amine groups
tCNO: tricoordinate binding by carboxylate, amine and alkoxide groups
tCP: tricoordinate binding by carboxylate monodentately and bidentately by phosphate groups
tCNP: tricoordinate binding by carboxylate, amine and phosphate groups
tCNbP: tetracoordinate binding by carboxylate and amine groups monodentately and bidentately by phosphate group
DI: Delocalitation index

Acknowledgments

The authors would like to thank the technical and human support provided by the IZO-SGI SGIker of UPV/EHU and European funding (ERDF and ESF). Financial support comes from UPV/EHU (PES14/35), Eusko Jaurlaritza (IT588-13) and the Spanish Ministerio de Ciencia e Innovación (CTQ2015-67608-P).

Appendix A. Supplementary data

Supplementary data to this article can be found online at https://doi.org/10.1016/j.jinorgbio.2018.12.004.

References

[1] C. Exley, A biogeochemical cycle for aluminium? J. Inorg. Biochem. 97 (1) (2003) 1–7, https://doi.org/10.1016/S0162-0134(03)00274-5.
[2] C. Exley, Darwin, natural selection and the biological essentiality of aluminium and silicon, Trends Biochem. Sci. 34 (12) (2009) 589–593, https://doi.org/10.1016/j.tibs.2009.07.006.
[3] C. Exley, The coordination chemistry of aluminium in neurodegenerative disease, Coord. Chem. Rev. 256 (19-20) (2012) 2142–2146, https://doi.org/10.1016/j.ccr.2012.02.020.
[4] T. MacDonald, R. Martin, Aluminum ion in biological systems, Trends Biochem. Sci.

13 (1988) 15–19, https://doi.org/10.1016/0968-0004(88)90012-6.
[5] Bharathi, P. Vasudevaraju, M. Govindaraju, A. Palanisamy, K. Sambamurti, K. Rao, Molecular toxicity of aluminium in relation to neurodegeneration, Indian J. Med. Res. 128 (2008) 545–556.
[6] C. Shaw, L. Tomljenovic, Aluminum in the central nervous system (CNS): toxicity in humans and animals, vaccine adjuvants, and autoimmunity, Immunol. Res. 56 (2-3) (2013) 304–316, https://doi.org/10.1007/s12026-013-8403-1.
[7] C. Exley, The pro-oxidant activity of aluminum, Free Radical Biol. Med. 36 (3) (2004) 380–387, https://doi.org/10.1016/j.freeradbiomed.2003.11.017.
[8] J. Mujika, F. Ruipérez, I. Infante, J. Ugalde, C. Exley, X. Lopez, Pro-oxidant activity of aluminum: stabilization of the aluminum superoxide radical ion, J. Phys. Chem. A 115 (24) (2011) 6717–6723, https://doi.org/10.1021/jp203290b.
[9] F. Ruipérez, J. Mujika, J. Ugalde, C. Exley, X. Lopez, Pro-oxidant activity of aluminum: promoting the Fenton reaction by reducing Fe(III) to Fe(II), J. Inorg. Biochem. 117 (0) (2012) 118–123, https://doi.org/10.1016/j.jinorgbio.2012.09.008.
[10] S. Cho, J. Joshi, Effect of long-term feeding of aluminium chloride on hexokinase and glucose-6-phosphate dehydrogenase in the brain, Toxicology 48 (1) (1988) 61–69, https://doi.org/10.1016/0300-483X(88)90059-5.
[11] C. Exley, J. Birchall, N. Price, Aluminum inhibition of hexokinase activity in vitro: a study in biological availability, J. Inorg. Biochem. 54 (4) (1994) 297–304, https://doi.org/10.1016/0162-0134(94)80035-9.
[12] G. Trapp, Studies of aluminium interaction with enzymes and proteins - the inhibition of hexokinase, Neurotoxicology 1 (4) (1980) 89–100.
[13] Z. Xu, L. Fox, S. Melethil, L. Winberg, M. Badr, Mechanism of aluminum-induced inhibition of hepatic glycolysis - inactivation of phosphofructokinase, J. Pharmacol. Exp. Ther. 254 (1) (1990) 301–305.
[14] J. Mujika, J. Ugalde, X. Lopez, Aluminum interaction with glutamate and α-Ketoglutarate: a computational study, J. Phys. Chem. B 118 (24) (2014) 6680–6686, https://doi.org/10.1021/jp502724w.
[15] S. Yang, J. Huh, J. Lee, S. Choi, T. Kim, S. Cho, Inactivation of human glutamate dehydrogenase by aluminum, Cell. Mol. Life Sci. 60 (11) (2003) 2538–2546, https://doi.org/10.1007/s00018-003-3298-y.
[16] E. Formoso, J. Mujika, S. Grabowski, X. Lopez, Aluminum and its effect in the equilibrium between folded/unfolded conformation of NADH, J. Inorg. Biochem. 152 (2015) 139–146, https://doi.org/10.1016/j.jinorgbio.2015.08.017.
[17] T. Kiss, From coordination chemistry to biological chemistry of aluminium, J. Inorg. Biochem. 128 (2013) 156–163, https://doi.org/10.1016/j.jinorgbio.2013.06.013.
[18] E. Rezabal, J. Mercero, X. Lopez, J. Ugalde, A study of the coordination shell of aluminum(III) and magnesium(II) in model protein environments: thermodynamics of the complex formation and metal exchange reactions, J. Inorg. Biochem. 100 (3) (2006) 374–384, https://doi.org/10.1016/j.jinorgbio.2005.12.007.
[19] E. Rezabal, J. Mercero, X. Lopez, J. Ugalde, A theoretical study of the principles regulating the specificity for Al(III) against Mg(II) in protein cavities, J. Inorg. Biochem. 101 (9) (2007) 1192–1200, https://doi.org/10.1016/j.jinorgbio.2007.06.010.
[20] E. Rezabal, J. Mercero, X. Lopez, J. Ugalde, Protein side chains facilitate Mg/Al exchange in model protein binding sites, Chem. Phys. Chem. 8 (14) (2007) 2119–2124, https://doi.org/10.1002/cphc.200700335.
[21] J. Fan, L. He, J. Liu, M. Tang, Investigation on the micro-mechanisms of Al^{3+} interfering the reactivities of aspartic acid and its biological processes with Mg^{2+}, J. Mol. Model. 16 (2010) 1639–1650, https://doi.org/10.1007/s00894-010-0676-x.
[22] J. Mujika, J. Ugalde, X. Lopez, Computational evaluation of pK_a for oxygenated side chain containing amino acids interacting with aluminum, Theor. Chem. Acc. 128 (2011) 477–484, https://doi.org/10.1007/s00214-010-0807-6.
[23] A. Oliveira de Noronha, L. Guimarães, H. Duarte, Structural and thermodynamic analysis of the first mononuclear aqueous aluminum citrate complex using DFT calculations, J. Chem. Theory Comput. 3 (3) (2007) 930–937, https://doi.org/10.1021/ct700016f.
[24] N. Luque, J. Mujika, E. Rezabal, J. Ugalde, X. Lopez, Mapping the affinity of aluminum(III) for biophosphates: interaction mode and binding affinity in 1: 1 complexes, Phys. Chem. Chem. Phys. 16 (2014) 20107–20119, https://doi.org/10.1039/C4CP02770A.
[25] M. Hémadi, G. Miquel, P. Kahn, J. Chahine, Aluminum exchange between citrate and human serum transferrin and interaction with transferrin receptor 1, Biochemistry 42 (10) (2003) 3120–3130, https://doi.org/10.1021/bi020627p.
[26] K. Atkári, T. Kiss, R. Bertani, R. Martin, Interactions of aluminum(III) with phosphates, Inorg. Chem. 35 (24) (1996) 7089–7094, https://doi.org/10.1021/ic960329e.
[27] T. Kiss, P. Zatta, B. Corain, Interaction of aluminium (III) with phosphate-binding sites: biological aspects and implications, Coord. Chem. Rev. 149 (1996) 329–346, https://doi.org/10.1016/S0010-8545(96)90036-3.
[28] D. Mazzuca, N. Russo, M. Toscano, A. Grand, On the interaction of bare and hydrated aluminum ion with nucleic acid bases (U, T, C, A, G) and monophosphate nucleotides (UMP, dTMP, dCMP, dAMP, dGMP), J. Phys. Chem. B 110 (17) (2006) 8815–8824, https://doi.org/10.1021/jp055223w.
[29] R. Grande-Aztatzi, E. Formoso, J. Mujika, J. Ugalde, X. Lopez, Phosphorylation promotes Al(III) binding to proteins: GEGEGSGG as a case study, Phys. Chem. Chem. Phys. 18 (2016) 7197–7207, https://doi.org/10.1039/C5CP06379E.
[30] E. Formoso, X. Lopez, A computational study on the aluminum interaction with D-glucose 6-phosphate in various stoichiometries, RSC Adv. 7 (2017) 6064–6079, https://doi.org/10.1039/c6ra27037a.
[31] V. Gupta, S. Anitha, M. Hegde, L. Zecca, R. Garruto, R. Ravid, S. Shankar, R. Stein, P. Shanmugavelu, K. Jagannatha Rao, Aluminium in Alzheimer's disease: are we still at a crossroad? Cell. Mol. Life Sci. 62 (2) (2005) 143–158, https://doi.org/10.1007/s00018-004-4317-3.
[32] V. Kumar, K. Gill, Aluminium neurotoxicity: neurobehavioural and oxidative aspects, Arch. Toxicol. 83 (11) (2009) 965–978, https://doi.org/10.1007/s00204-009-0455-6.
[33] C. Exley, N. Price, S. Kelly, J. Birchall, An interaction of β-amyloid with aluminium in vitro, FEBS Lett. 324 (3) (1993) 293–295, https://doi.org/10.1016/0014-5793(93)80137-J.
[34] M. Kawahara, M. Kato-Negishi, Link between aluminum and the pathogenesis of Alzheimer's disease: the integration of the aluminum and amyloid cascade hypotheses, Int. J. Alzheimers Dis. (2011), https://doi.org/10.4061/2011/276393.
[35] P. Mantyh, J. Ghilardi, S. Rogers, E. DeMaster, C. Allen, E. Stimson, J. Maggio, Aluminum, iron, and zinc ions promote aggregation of physiological concentrations of β-Amyloid peptide, J. Neurochem. 61 (3) (1993) 1171–1174, https://doi.org/10.1111/j.1471-4159.1993.tb03639.x.
[36] S. Yumoto, S. Kakimi, A. Ohsaki, A. Ishikawa, Demonstration of aluminum in amyloid fibers in the cores of senile plaques in the brains of patients with Alzheimer's disease, J. Inorg. Biochem. 103 (11) (2009) 1579–1584, https://doi.org/10.1016/j.jinorgbio.2009.07.023.
[37] M. Abdel-Ghany, A. El-Sebae, D. Shalloway, Aluminum-induced nonenzymatic phospho-incorporation into human tau and other proteins, J. Biol. Chem. 268 (16) (1993) 11976–11981.
[38] G. Fasman, Aluminum and Alzheimer's disease: model studies, Coord. Chem. Rev. 149 (1996) 125–165, https://doi.org/10.1016/S0010-8545(96)90020-X.
[39] L. Pizer, Enzymology and regulation of serine biosynthesis in cultured human cells, J. Biol. Chem. 239 (1964) 4219–4226.
[40] E. Kiss, A. Lakatos, I. Bányai, T. Kiss, Interactions of Al(III) with phosphorylated amino acids, J. Inorg. Biochem. 69 (3) (1998) 145–151, https://doi.org/10.1016/S0162-0134(97)10011-3.
[41] M. Mohan, E. Abbott, Metal complexes of amino acid phosphate esters, Inorganic Chemistry 17 (8) (1978) 2203–2207, https://doi.org/10.1021/ic50186a036.
[42] M. Mohan, D. Bancroft, E. Abbott, Mixed-ligand complexes of O-phospho-DL-serine, Inorg. Chem. 18 (9) (1979) 2468–2472, https://doi.org/10.1021/ic50199a028.
[43] N. Luque, J. Mujika, E. Formoso, X. Lopez, Aluminum interaction with 2-3-diphosphoglyceric acid. A computational study. RSC Adv. 5 (78) (2015) 63874–63881, https://doi.org/10.1039/C5RA06796K.
[44] J. Tomasi, B. Mennucci, R. Cammi, Quantum mechanical continuum solvation models, Chem. Rev. 105 (8) (2005) 2999–3094, https://doi.org/10.1021/cr9904009.
[45] M. Frisch, G. Trucks, H. Schlegel, G. Scuseria, M. Robb, J. Cheeseman, G. Scalmani, V. Barone, B. Mennucci, G. Petersson, H. Nakatsuji, M. Caricato, X. Li, H. Hratchian, A. Izmaylov, J. Bloino, G. Zheng, J. Sonnenberg, M. Hada, M. Ehara, K. Toyota, R. Fukuda, J. Hasegawa, M. Ishida, T. Nakajima, Y. Honda, O. Kitao, H. Nakai, T. Vreven, J. J. A. Montgomery, J. Peralta, F. Ogliaro, M. Bearpark, J. Heyd, E. Brothers, K. Kudin, V. Staroverov, R. Kobayashi, J. Normand, K. Raghavachari, A. Rendell, J. Burant, S. Iyengar, J. Tomasi, M. Cossi, N. Rega, J. Millam, M. Klene, J. Knox, J. Cross, V. Bakken, C. Adamo, J. Jaramillo, R. Gomperts, R. Stratmann, O. Yazyev, A. Austin, R. Cammi, C. Pomelli, J. Ochterski, R. Martin, K. Morokuma, V. Zakrzewski, G. Voth, P. Salvador, J. Dannenberg, S. Dapprich, A. Daniels, O. Farkas, J. Foresman, J. Ortiz, J. Cioslowski,D. Fox, Gaussian 09, Revision A.02, 2009.
[46] A.D. Becke, Density-functional exchange-energy approximation with correct asymptotic behavior, Phys. Rev. A. 38 (1988) 3098–3100.
[47] A.D. Becke, Density-functional thermochemistry. III. The role of exact exchange, J. Chem. Phys. 98 (1993) 5648–5652.
[48] C. Lee, W. Yang, R.G. Parr, Development of the Colle-Salvetti correlation-energy formula into a functional of the electron density, Phys. Rev. B. 37 (1988) 785–789.
[49] S. Vosko, L. Wilk, M. Nusair, Accurate spin-dependent electron liquid correlation energies for local spin density calculations: a critical analysis, Can. J. Phys. 58 (1980) 1200.
[50] S. Grimme, S. Ehrlich, L. Goerigk, Effect of the damping function in dispersion corrected density functional theory, J. Comput. Chem. 32 (2011) 1456–1465, https://doi.org/10.1002/jcc.21759.
[51] J. Ali-Torres, L. Rodriguez-Santiago, M. Sodupe, Computational calculations of pKa values of imidazole in Cu(II) complexes of biological relevance, Phys. Chem. Chem. Phys. 13 (2011) 7852-Ű7861, https://doi.org/10.1039/C0CP02319A.
[52] W. Haynes, CRC Handbook of Chemistry and Physics, CRC Press, 2015.
[53] M. Śmiechowski, Theoretical pKa prediction of O-phosphoserine in aqueous solution, Chem. Phys. Lett. 501 (1-3) (2010) 123–129, https://doi.org/10.1016/j.cplett.2010.10.063.
[54] C. Matta, R. Boyd, The Quantum Theory of Atoms in Molecules: From Solid State to DNA and Drug Design, (2007).
[55] A.Todd, T. Keith, AIMAll (Version 11.08.23), Gristmill Software, Overland Park KS, USA, (aim.tkgristmill.com) (2011).
[56] W. Humphrey, A. Dalke, K. Schulten, VMD: visual molecular dynamics, J. Mol. Graph. 14 (1) (1996) 33-Ű38, https://doi.org/10.1016/0263-7855(96)00018-5.
[57] S. Grabowski, What is the covalency of hydrogen bonding? Chem. Rev. 111 (4) (2011) 2597–2625, https://doi.org/10.1021/cr800346f.